JACS
JOURNAL OF THE AMERICAN CHEMICAL SOCIETY
Communication
pubs.acs.org/JACS

NCN Pincer–Pt Complexes Coordinated by (Nitronyl Nitroxide)-2-ide Radical Anion

Xun Zhang, Shuichi Suzuki, Masatoshi Kozaki, and Keiji Okada*

Department of Chemistry, Graduate School of Science, Osaka City University, Sugimoto, Sumiyoshi-ku, Osaka 558-8585, Japan

Supporting Information

ABSTRACT: New pincer–Pt complexes coordinated by (nitronyl nitroxide)-2-ide radical anion were prepared as stable compounds in high yields. The structures of these Pt complexes and the oxidized complexes were unequivocally determined by spectral and crystal structure analyses. The oxidation potential of the nitronyl nitroxide moiety in these complexes was shifted in the negative direction by ~0.6 V as a result of coordination to the Pt(II) atom.

Open-shell molecules have attracted intense attention in materials science. For instance, high-spin organic molecules with large exchange interactions,[1] molecule-based magnets,[2,3] radical-based batteries,[4] and materials exhibiting unique electronic and spintronic properties[5,6] have been investigated. In these studies, nitronyl nitroxides (**NN-Rs**) are widely used as stable spin sources.[1−3,5] Composite systems involving magnetic metal ions and **NN-Rs** as ligative spin sources have also been extensively investigated.[2] However, only a few studies of metal complexes coordinated by (nitronyl nitroxide)-2-ide radical anion (**NN-ML$_n$**; M = metal ion, L = ligand) have been reported. Leute and Ullman reported mercury complexes (**NN-HgOAc**, **NN$_2$-Hg**, and their analogues) as early as 1972.[7] Recently, detailed studies of these mercury complexes, including crystal structures and physicochemical properties, have been reported.[8,9] In connection with these studies, Weiss and Kraut prepared an interesting Pd complex coordinated by (nitrosonium nitroxide)-2-ide through a possible carbene intermediate.[10] The corresponding Pd complexes of **NN** radicals have not been reported. The nature of the carbon–metal bonding in **NN-ML$_n$** complexes should be highly dependent on the metal ion. However, **NN-ML$_n$** complexes with metals other than mercury(II) have virtually not been reported.[11] In this paper, we report the synthesis and characterization of new pincer–Pt complexes **1** and **2** coordinated by (nitronyl nitroxide)-2-ide radical anion. We found that the oxidation potential of the **NN** moiety is shifted in the negative direction to a remarkable extent (~0.6 V) as a result of coordination to the Pt(II) atom.

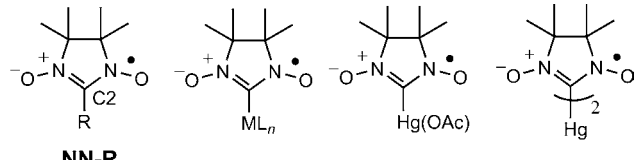

NN-R (R = H, Ph, NMe$_2$) **NN-ML$_n$** **NN-Hg(OAc)** **NN$_2$-Hg**

Compound **1** was readily prepared (94% yield) by treating a mixture of **Pt(NCN)Cl** and **NN-H** (1 equiv) with *n*Bu$_4$NOH (as a 37% methanol solution, 1.8 equiv) in 1:1 (v/v) dichloromethane/methanol at room temperature for 1 h (Scheme 1). Complex **1** was found to be stable toward air and moisture. Compound **2** was also prepared in good yield [see the Supporting Information (SI)]. As a reference, compound **3** with remote platinization via a phenylene ethynylene spacer was prepared according to the established procedure.[11d,12]

Scheme 1. Synthesis of 1 and Structures of 2 and 3

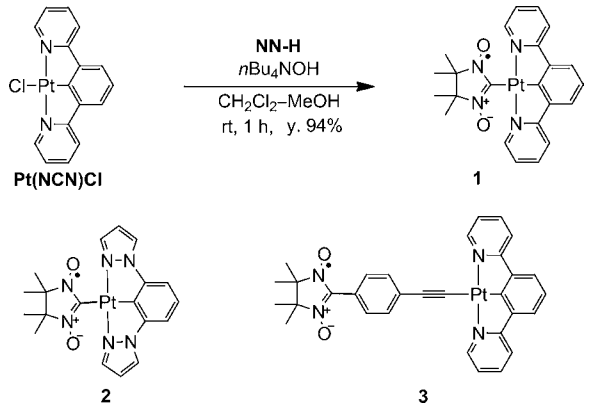

The crystal structures of **1** and **2** are shown in Figure 1(I) and Figure S1 in the SI, respectively.[13] The length of the Pt–C bond in **1** [2.11 Å; bond **c** in Figure 1(I)] is similar to that in

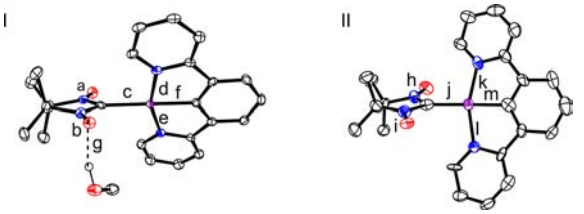

Figure 1. Crystal structures of (I) **1** and (II) cationic **NN$^+$-Pt(NCN)-1** (**1**$^+$). Selected bond lengths (Å) in (I): **a** (N–O), 1.300; **b** (N–O), 1.308; **c** (Pt–C), 2.106; **d** (Pt–N), 2.053; **e** (Pt–N), 2.046; **f** (Pt–C), 1.944; **g** (O···H), 1.765. In (**II**): **h** (N–O), 1.230, 1.270; **i** (N–O), 1.250, 1.215; **j** (Pt–C), 2.073, 2.067; **k** (Pt–N), 2.082, 2.043; **l** (Pt–N), 2.076, 2.072; **m** (Pt–C), 1.942, 1.956.

Received: August 18, 2012
Published: October 17, 2012

dx.doi.org/10.1021/ja308103g | J. Am. Chem. Soc. 2012, 134, 17866–17868

the related NCN Pt imidazole carbene complexes (2.09 Å).[14] The torsion angle between the **NN** plane (defined by O−N═C−N−O) and the central phenylene plane in the NCN pincer ligand is 59°. Methanol is involved as a crystallization solvent bound to the **NN** moiety by a hydrogen bond (N−O···HOCH$_3$, with experimentally observed distances $r_{O\cdots H}$ = 1.77 Å and r_{O-O} = 2.74 Å).

This hydrogen bond seems to play an important role in the solubility. The solubility of **1** was very poor in polar aprotic solvents such as dichloromethane, acetone, and acetonitrile. Interestingly, however, the solubility increased remarkably upon the addition of a few drops of a protic solvent such as methanol, ethanol, or water. We assume that the change in solubility of **1** is due to the hydrogen bonding with the protic solvent. Recrystallization of **1** from dichloromethane/ethanol and acetonitrile/water mixtures selectively captured ethanol and water, respectively as crystalline solvent molecules (Figure S2). The shape of the absorption spectrum was also influenced by the addition of a small amount of methanol (Figure S3). The observed spectral change can be qualitatively explained by the hydrogen bond observed in the X-ray analysis. Time-dependent density functional theory (TDDFT) calculations for **1** with and without methanol qualitatively accounted for the relative sequence of energies of absorptions and number of major peaks, although the calculated energies were considerably higher than the observed energies for all transitions (Figure S3).

The electron spin resonance (ESR) spectrum of **1** measured in degassed dichloromethane at room temperature (Figure 2)

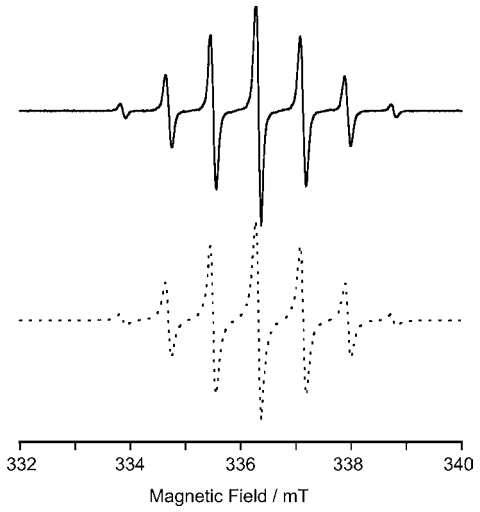

Figure 2. ESR spectra of **1** in dichloromethane at room temperature. The solid and dotted lines show the observed and simulated spectra, respectively. Parameters for the simulation: g = 2.0062 (ν_0 = 9.443659 GHz), $|a_{Pt}|$ = 1.655 mT, and $|a_N|$ = 0.811 mT.

showed seven split lines with g = 2.0062. The spectrum was simulated using the following parameters: $|a_N|$ = 0.811 mT split by two equivalent ^{14}N nuclei (I = 1) and $|a_{Pt}|$ = 1.655 mT split by a ^{195}Pt nucleus (I = $^1/_2$, natural abundance = 33.7%). The ESR spectra of **2** and **3** are shown in Figure S4. Compound **2** has a similar but slightly larger $|a_{Pt}|$ value (1.700 mT). Obviously, no hyperfine coupling of $|a_{Pt}|$ was observed for **3**.

Compound **1** exhibited unique characteristics in regard to its oxidation potential. A reversible redox wave was observed at −0.19 V vs Fc/Fc$^+$ for **1** in dichloromethane (−0.21 V vs Fc/Fc$^+$ for **2**) (Table 1). The observed waves in **1** and **2** cannot be ascribed to oxidation of Pt(II), since the reference **Pt(NCN)Cl**

Table 1. First Oxidation Potentials of 1, 2, and Reference Compounds

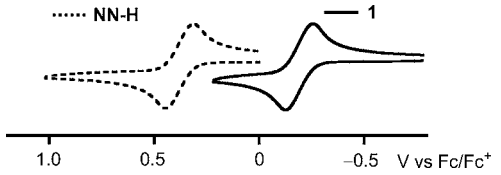

compound	E_{ox} (V vs Fc/Fc$^+$)[a]
1	−0.19
2	−0.21
3	+0.36
NN-Hg(OAc)	+0.21
NN$_2$-Hg	+0.18
NN-H	+0.38
NN-Ph	+0.37
NN-NMe$_2$	+0.11

[a]Measured in dichloromethane with 0.1 M nBu$_4$NClO$_4$. Note: 0 V vs Fc/Fc$^+$ = +0.48 V vs SCE. All waves were reversible waves.

showed a much higher irreversible oxidation wave at around +0.47 V vs Fc/Fc$^+$. However, they could be assigned to the oxidation of the **NN** moiety, which generally shows a reversible oxidation wave in a much more positive voltage region (e.g., +0.38 V vs Fc/Fc$^+$ for **NN-H** and +0.37 V vs Fc/Fc$^+$ for **NN-Ph**). The oxidation potentials of **1** and **2** were markedly shifted in the negative direction (by ∼0.6 V) compared with **NN-H** and **NN-Ph**. In contrast to **1** and **2**, remote-platinized **3** showed an oxidation wave in the normal region (+0.36 V vs Fc/Fc$^+$). The oxidation potentials of **1** and **2** were much lower than those of electron-rich **NN-NMe$_2$** and the mercury compounds **NN-HgOAc** and **NN$_2$-Hg.** These results clearly demonstrate the unique characteristics of the **NN-Pt** complexes **1** and **2**.[15]

The lower oxidation potential of **2** relative to **1** may suggest stronger π-donating ability of the Pt ion in **2**. This consideration is supported by the slightly larger $|a_{Pt}|$ value (Figure 2) and the shorter Pt−C (**NN**) bond length in **2** (2.06 Å vs 2.11 Å in **1**; Figure 1 and Figure S1).

To obtain conclusive evidence about the electronic structure of the oxidized state, we carried out chemical oxidation of **1** using a one-electron-oxidation reagent, tris(p-bromophenyl)-ammonium hexafluorophosphate (TBPA·PF$_6$). Treatment of a dichloromethane solution of **1** [**NN-Pt(NCN)-1**] with 1 equiv of TBPA·PF$_6$ gave **1**$^+$ [**NN**$^+$**-Pt(NCN)-1**] in good yield (88%). The structure was confirmed by mass spectrometry, ^{1}H NMR spectroscopy, elemental analysis, and X-ray crystal structure analysis. The observation of ^{1}H NMR signals (Figure S6) clearly shows the diamagnetic nature of **1**$^+$. In the crystal structure analysis, two structurally similar but independent molecules were observed in the unit cell. The structure of one of them is shown in Figure 1(II).[13] The Pt−C (**NN**) bond length of 2.07 Å is shorter than that in neutral **1** (2.11 Å). The torsion angle (55°, 57°) between the **NN**$^+$ plane and the central phenylene plane of the **NCN** ligand is similar to but slightly smaller than that in neutral **1** (59°). Importantly, the observed N−O bond lengths (1.22−1.27 Å) in **1**$^+$ are clearly shorter than those in neutral **1** (1.30 Å) and similar to those of nitrosonium nitroxide (typically 1.23 Å).[10,16] Thus, the one-electron-

dx.doi.org/10.1021/ja308103g | J. Am. Chem. Soc. 2012, 134, 17866−17868

oxidized species $\mathbf{1}^+$ clearly contains nitrosonium nitroxide, as denoted in the formula **NN$^+$-Pt(NCN)-1**.

In summary, we have prepared new pincer−Pt complexes coordinated by (nitronyl nitroxide)-2-ide radical anions. The oxidation potentials of the nitronyl nitroxide moiety in these complexes were strongly shifted in the negative direction (by ∼0.6 V) by the direct coordination to the Pt atom, while the reversibility was maintained. The clarification and application of this strong metal perturbation in anionic metalloid π systems are in progress.

■ ASSOCIATED CONTENT

Ⓢ Supporting Information

Experimental and computational procedures, crystal structure of **2** (Figure S1), crystal structures of **1** with hydrogen-bonded ethanol or water (Figure S2), absorption spectral changes of **1** in the 400−600 nm region induced by the addition of a small amount of methanol (Figure S3), ESR spectra of **2** and **3** (Figure S4), crystal structures of the two independent molecules in $\mathbf{1}^+$ (Figure S5), ^{1}H NMR spectrum of $\mathbf{1}^+$ (Figure S6), and HMQC and HMBC spectra of $\mathbf{1}^+$ (Figure S7). This material is available free of charge via the Internet at http://pubs.acs.org.

■ AUTHOR INFORMATION

Corresponding Author

okadak@sci.osaka-cu.ac.jp

Notes

The authors declare no competing financial interest.

■ ACKNOWLEDGMENTS

This work was supported by grants from JSPS (22350066 to K.O.) and from the Sumitomo Foundation and the Tokuyama Science Foundation (to S.S.).

■ REFERENCES

(1) For instance, see: (a) Rajca, A.; Olankitwanit, A.; Rajca, S. *J. Am. Chem. Soc.* **2011**, *133*, 4750−4753. (b) Suzuki, S.; Furui, T.; Kuratsu, M.; Kozaki, M.; Shiomi, D.; Sato, K.; Takui, T.; Okada, K. *J. Am. Chem. Soc.* **2010**, *132*, 15908−15910. (c) Hiraoka, S.; Okamoto, T.; Kozaki, M.; Shiomi, D.; Sato, K.; Takui, T.; Okada, K. *J. Am. Chem. Soc.* **2004**, *126*, 58−59. (d) Mukai, K.; Ishizu, K.; Nakahara, M.; Deguchi, Y. *Bull. Chem. Soc. Jpn.* **1980**, *53*, 3363−3364.

(2) (a) Kahn, O. *Molecular Magnetism*; VCH: New York, 1993; pp 1−380. (b) *Magnetism: Molecules to Materials II−IV*; Miller, J. S., Drillon, M., Eds.; Wiley-VCH: New York, 2001−2005. (c) Gatteschi, D.; Sessoli, R.; Villain, J. *Molecular Nanomagnets*; Oxford University Press: New York, 2006; pp 1−395.

(3) (a) Masuda, Y.; Kuratsu, M.; Suzuki, S.; Kozaki, M.; Shiomi, D.; Sato, K.; Takui, T.; Hosokoshi, Y.; Lan, X.-Z.; Miyazaki, Y.; Inaba, A.; Okada, K. *J. Am. Chem. Soc.* **2009**, *131*, 4670−4673. (b) Kuratsu, M.; Suzuki, S.; Kozaki, M.; Shiomi, D.; Sato, K.; Takui, T.; Kanazawa, T.; Hosokoshi, Y.; Lan, X.-Z; Miyazaki, Y.; Inaba, A.; Okada, K. *Chem.—Asian J.* **2012**, *7*, 1604−1609.

(4) (a) Nishide, H.; Oyaizu, K. *Science* **2008**, *319*, 737−738. (b) Morita, Y.; Nishida, S.; Murata, T.; Moriguchi, M.; Ueda, A.; Satoh, M.; Arifuku, K.; Sato, K.; Takui, T. *Nat. Mater.* **2011**, *10*, 947−951.

(5) (a) Pal, S. K.; Itkis, M. E.; Tham, F. S.; Reed, R. W.; Oakley, R. T.; Haddon, R. C. *Science* **2005**, *309*, 281−284. (b) Iwasaki, A.; Hu, L.; Suizu, R.; Nomura, K.; Yoshikawa, H.; Awaga, K.; Noda, Y.; Kanai, K.; Ouchi, Y.; Seki, K.; Ito, H. *Angew. Chem., Int. Ed.* **2009**, *48*, 4022−4024.

(6) (a) Matsushita, M. M.; Kawakami, H.; Sugawara, T.; Ogata, M. *Phys. Rev. B* **2008**, *77*, No. 195208. (b) Komatsu, H.; Matsushita, M. M.; Yamamura, S.; Sugawara, Y.; Suzuki, K.; Sugawara, T. *J. Am. Chem. Soc.* **2010**, *132*, 4528−4529. (c) Sugawara, T.; Komatsu, H.; Suzuki, K. *Chem. Soc. Rev.* **2011**, *40*, 3105−3118.

(7) Leute, R. K.; Ullman, E. F. U.S. Patent 3,697,535, 1969.

(8) Weiss, R.; Kraut, N.; Hampel, F. *J. Organomet. Chem.* **2001**, *617−618*, 473−482.

(9) Fokin, S. V.; Romanenko, G. V.; Baumgarten, M.; Ovcharenko, V. I. *J. Struct. Chem.* **2003**, *44*, 864−869.

(10) Weiss, R.; Kraut, N. *Angew. Chem., Int. Ed.* **2002**, *41*, 311−314.

(11) (a) Clark, H. C.; Wong, C. S. *J. Am. Chem. Soc.* **1977**, *99*, 7073−7074. (b) Milaeva, E. R.; Rubezhov, A. Z.; Prokoph'ev, A. I.; Milaeva, A. G.; Okhlobystin, O. Y. *J. Organomet. Chem.* **1980**, *188*, C43−C45. (c) Milaeva, E. R.; Shpakovsky, D. B.; Shaposhnikova, E. N.; Grigor'ev, E. V.; Berberova, N. T.; Egorov, M. P. *Russ. Chem. Bull.* **2001**, *50*, 716−719. (d) Stroh, C.; Mayor, M.; von Hänisch, C.; Turek, P. *Chem. Commun.* **2004**, 2050−2051. (e) Kusamoto, T.; Kume, S.; Nishihara, H. *J. Am. Chem. Soc.* **2008**, *130*, 13844−13845. (f) McKinnon, S. D. J.; Gilroy, J. B.; McDonald, R.; Patrick, B. O.; Hicks, R. G. *J. Mater. Chem.* **2011**, *21*, 1523−1530.

(12) (a) Paw, W.; Cummings, S. D.; Mansour, M. A.; Connick, W. B.; Geiger, D. K.; Eisenberg, R. *Coord. Chem. Rev.* **1998**, *171*, 125−150. (b) *The Chemistry of Pincer Compounds*; Morales-Morales, D., Jensen, C. M., Eds.; Elsevier: Tokyo, 2008; pp 1−450. (c) Yoshida, K.; Yamaguchi, S.; Osuka, A.; Shinokubo, H. *Organometallics* **2010**, *29*, 3997−4000.

(13) Crystallographic data for **1**: monoclinic, space group $P2_1/n$ (No. 14), a = 9.8985(12) Å, b = 15.6407(19) Å, c = 14.4655(18) Å, β = 97.590(3)°, V = 2219.9(5) Å^3, Z = 4, ρ_{calc} = 1.839 g cm^{-3}, T = 150(2) K, R = 0.0360, wR = 0.0621, GOF = 1.186 (CCDC entry 895137). Crystallographic data for $\mathbf{1}^+\cdot\mathbf{PF_6}^-$: orthorhombic, space group $Pna2_1$ (No. 33), a = 29.7963(16) Å, b = 8.4080(5) Å, c = 21.7444(11) Å, V = 5447.6(5) Å^3, Z = 8, ρ_{calc} = 1.878 g cm^{-3}, T = 150(2) K, R = 0.0657, wR = 0.1243, GOF = 1.092 (CCDC entry 895138). Crystallographic data for **2**: monoclinic, space group $P2_1/n$ (No. 14), a = 8.9700(18) Å, b = 18.360(4) Å, c = 15.800(3) Å, β = 91.340(5)°, V = 2601.4(10) Å^3, Z = 4, ρ_{calc} = 1.865 g cm^{-3}, T = 150(2) K, R = 0.0476, wR = 0.0932, GOF = 1.072 (CCDC entry 895139).

(14) Li, K.; Chen, Y.; Lu, W.; Zhu, N.; Che, C.-M. *Chem.—Eur. J.* **2011**, *17*, 4109−4112.

(15) In a related system, the SOMO−HOMO level conversion of a ditholate−Pt complex has been reported (see ref 11e).

(16) Caneschi, A.; Laugier, J.; Rey, P. *J. Chem. Soc., Perkin Trans. 1* **1987**, 1077−1079.